Time-dependent polarimetric response and identifiability of localized energy deposition in irradiated Kerr plasmas

Jingxu Wu[1] · Zhengnan Zhang[2] (presenter) · Xiatong Li[3]

[1,2,3] Lomonosov Moscow State University, Moscow, Russia

[1] wuxj@my.msu.ru · [2] n2994208@gmail.com · [3] be2312701251@gmail.com

Physical model and research question

Irradiated Kerr inflow. We ask whether localized energy deposition has a distinguishable polarimetric signature in a thin, equatorial inflow on a fixed Kerr background. The prescribed density profile in Eq. (1) uses the dimensionless radius $\bar{r} = r/r_g$ and a taper f_{tap} at both radial boundaries. The initial electron density $n_{e,0}$ follows from fully ionized ^{56}Fe. A prescribed inward hard-photon beam illuminates the gas. The photon energies entering the collision kernels are evaluated in the local fluid frame.

Nonthermal lepton kinetics. The state N contains the electron and positron populations on a kinetic-energy grid per initial electron. The unperturbed operator F_r in Eq. (2) includes Compton scattering, Bethe–Heitler pair production in the iron Coulomb field, two-photon annihilation, vertical lepton escape, adiabatic compression and synchrotron cooling. A cold-electron return term accounts for net charge lost through escape. The plotted benchmark uses ordered-field streaming, with proper escape rate $v/(4H)$ for particle speed v and half-thickness H.

Controlled deposition and response. The ^{56}Fe(γ,n)^{55}Fe channel provides a reference energy scale. We prescribe the deposited power P_{dep} as a Gaussian in radius, wrapped azimuth and Boyer–Lindquist coordinate time, with $\Delta\varphi_w$ the shortest azimuthal difference and ε_p the time-integrated input at the fixed pulse center. The radial source vanishes for $|r - r_p| > 6\sigma_r$. The operator W_r redistributes leptons in energy with pv weights. Along each streamline, the small spectral perturbation evolves under the baseline Jacobian J_0 in proper time τ. The factor $u^t = dt/d\tau$ converts the source from coordinate-time to proper-time power.

Retarded polarized transfer. Each vacuum Kerr ray samples up to three equatorial crossings. Eq. (4) gives the emission time, local frequency and effective Gaussian slab length, where g_j is the redshift factor and ϑ_j is the ray angle to the slab normal in the fluid frame. The transfer coefficients come from the nonthermal spectra and include synchrotron emission and absorption, Faraday rotation and conversion. The sum of the two spectra weights total and linear emission and Faraday conversion. Their difference weights intrinsic circular emission and Faraday rotation. We propagate the coherency matrix toward the camera in a parallel-transported basis. In Eq. (5), U_j is the layer propagator and J_j its emission contribution. Matched runs share the flow, field, irradiation and escape prescription. Assessing attribution requires testing whether changes in other plasma parameters can produce similar signatures.

Governing equations

$$n_b(\bar{r}) = n_{b,30}\sqrt{\frac{30(30^2+a_*^2)}{\bar{r}(\bar{r}^2+a_*^2)}}\,f_{\rm tap}(\bar{r}), \qquad n_{e,0} = \frac{26}{56}n_b \tag{1}$$

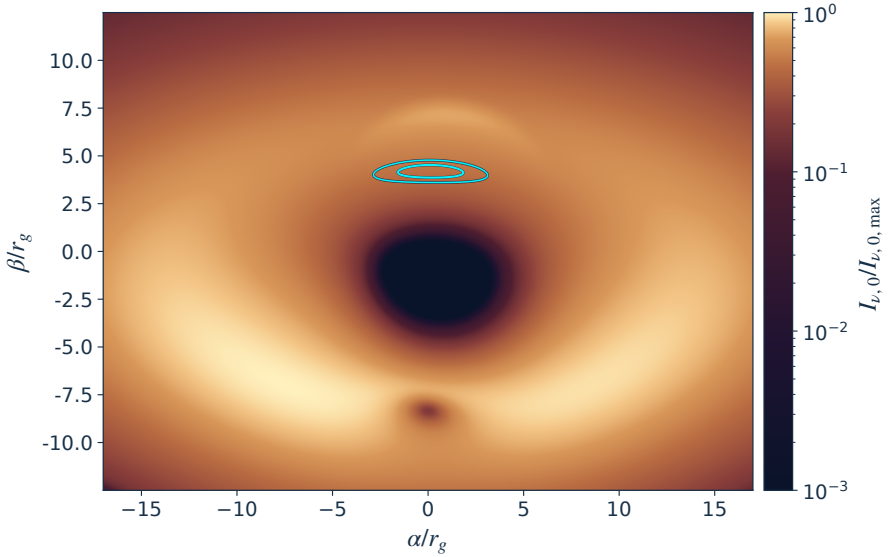
$$\frac{dN_0}{d\tau} = F_r(N_0), \qquad \frac{d\,\delta N}{d\tau} = J_0\,\delta N + u^t P_{\rm dep}\,W_r(N_0) \tag{2}$$

$$P_{\rm dep}(r,\phi,t) = \frac{\varepsilon_p}{\sqrt{2\pi}\,\sigma_t}\exp\left[-\frac{(r-r_p)^2}{2\sigma_r^2} - \frac{\Delta\phi_w^2}{2\sigma_\phi^2} - \frac{(t-t_p)^2}{2\sigma_t^2}\right], \quad |r-r_p| \le 6\sigma_r \tag{3}$$

$$t_{{\rm em},j} = (t_{\rm obs} - T_{\rm ref}) - (T_j - T_{\rm ref}), \qquad \nu_{{\rm loc},j} = \frac{\nu_\infty}{g_j}, \qquad \ell_j = \frac{\sqrt{2\pi}\,H_j}{|\cos\vartheta_j|} \tag{4}$$

$$C_j = U_j C_{j+1} U_j^\dagger + J_j, \qquad I_\nu = \mathrm{tr}\,C_0, \qquad \Delta I_\nu = I_{\nu,\,\rm pulse} - I_{\nu,0} \tag{5}$$

230 GHz brightness map and recomputed benchmark



BASELINE INTENSITY AND PULSE-INDUCED EXCESS. Color shows the no-pulse specific intensity at $\nu_\infty = 230$ GHz, normalized to its peak. The outer and inner cyan contours mark 50% and 80% of the peak positive ΔI_ν at $t_{\rm obs} - T_{\rm ref} = 1.75$ ms. The peak excess is 0.449 ppm of the peak baseline intensity. $T_{\rm ref} = 4.15862$ ms is the shortest crossing-to-camera travel time on the reference grid.

Geometry and gas. $M = 10$ solar masses, $a_* = 0.7$, $i = 60°$, $r_{\rm obs} = 100\ r_g$, and $H/r = 0.03$. The flow is evolved from 30 to 2.05 r_g, where $r_g = GM/c^2$ and $t_g = GM/c^3 = 0.0493$ ms. The untapered density normalization is $n_{b,30} = 10^{12}$ cm^{-3}. The equatorial field is $B = 50(30r_g/r)^2$ G.

Incident beam. The photon number density at 30 r_g is 10^{17} cm^{-3} in the fluid frame. The spectrum spans 16–156 MeV in the conserved energy E_∞, with an exponential scale of 30 MeV.

Gaussian pulse. The center (r_p, φ_p, t_p) is (8 r_g, 0, 0.98513 ms), with widths $(\sigma_r, \sigma_\varphi, \sigma_t) = (0.7\ r_g, 0.30$ rad, 0.19703 ms). The normalization is $\varepsilon_p = 10^{-4}$ MeV per initial electron.

Image sampling. The underlying image-plane grid is 352 × 352, with pixel spacing 0.0972 r_g. The plotted ranges are −17 to 17 in α/r_g and −12.5 to 12.5 in β/r_g. The Stokes maps are smoothed with a Gaussian kernel of FWHM 0.65 r_g.

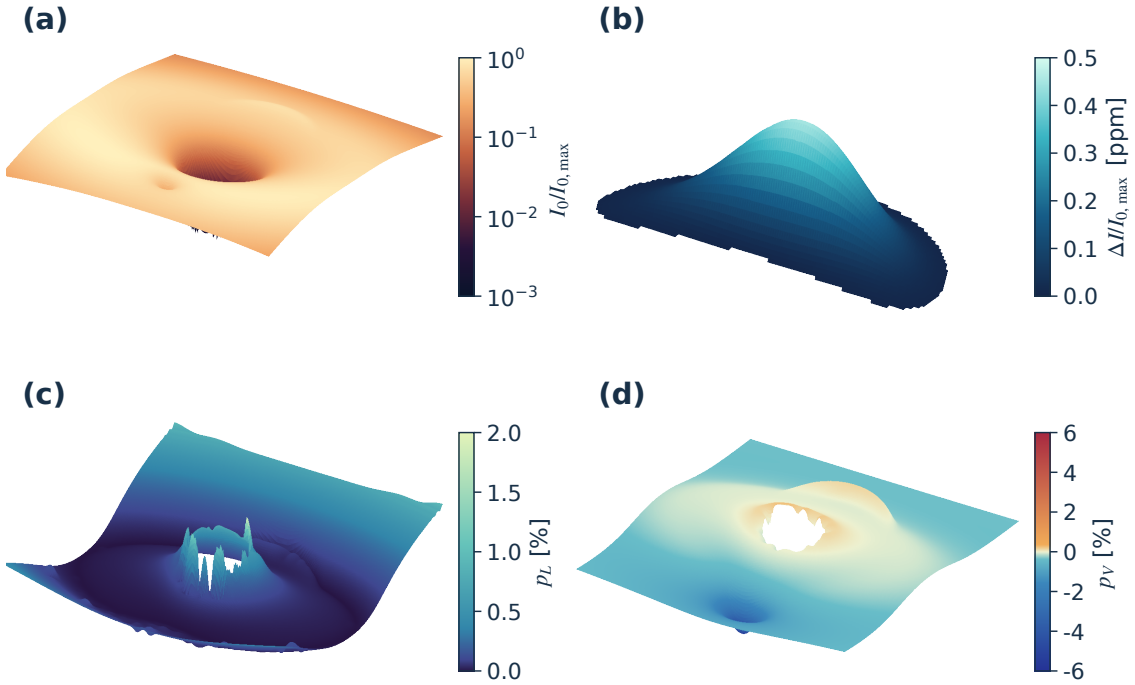
Time-dependent polarimetric response and identifiability of localized energy deposition in irradiated Kerr plasmas

Jingxu Wu[1] · Zhengnan Zhang[2] (presenter) · Xiatong Li[3]

[1,2,3] Lomonosov Moscow State University, Moscow, Russia

[1] wuxj@my.msu.ru · [2] n2994208@gmail.com · [3] be2312701251@gmail.com

230 GHz observer-plane surfaces



OBSERVER-PLANE SURFACES. All four panels use the ordered-field 230 GHz Stokes solution on the central 268 × 268 image-plane grid. The plotted heights encode observables on that grid.

(a) Baseline specific intensity. Color shows the ratio of the no-pulse intensity to its peak. Height shows the base-10 logarithm of that ratio.

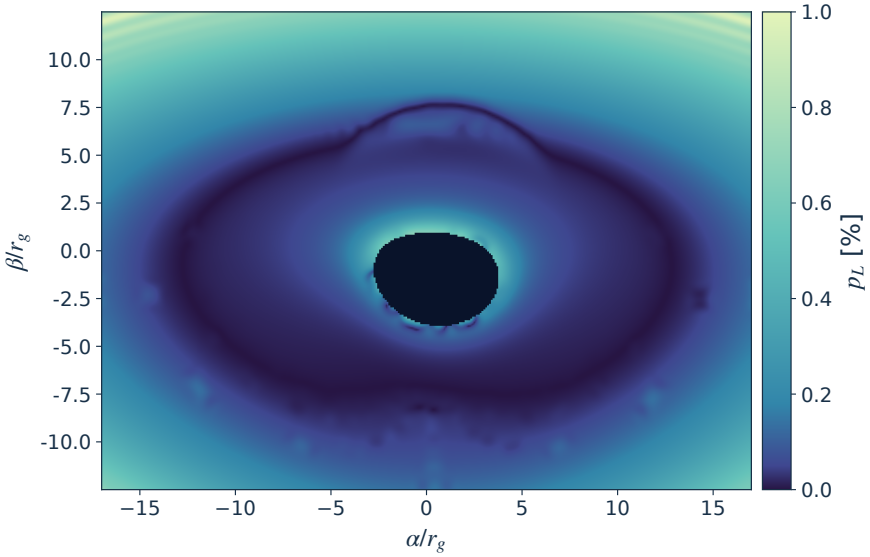
(b) Pulse-induced intensity excess. Color and height show the pulse-minus-baseline intensity, normalized to the baseline peak and expressed in ppm, at $t_{obs} - T_{ref} = 1.75$ ms. The crop shows $|\Delta I|$ at or above 1% of its peak.

(c) Baseline linear polarization fraction. Color shows $p_L = 100\sqrt{(Q_0^2 + U_0^2)}/I_0$ in percent. Height uses an inverse hyperbolic sine transform.

(d) Baseline circular polarization fraction. Color shows the signed ratio $p_V = 100\ V_0/I_0$ in percent, with the color transition centered at zero. Height uses a signed inverse hyperbolic sine transform.

Panels (a), (c) and (d) omit pixels below 0.1% of the peak baseline intensity. The color scales in (b)–(d) are linear.

230 GHz baseline linear polarization



BASELINE LINEAR POLARIZATION FRACTION. Color gives the local linear polarization fraction p_L at 230 GHz. The map uses the no-pulse solution and the same viewing geometry and display limits as the intensity map on page 1.

Image sampling. The 352 × 352 Stokes grid has a pixel spacing of 0.0972 r_g. The Stokes components are smoothed in the image plane with a Gaussian kernel of FWHM 0.65 r_g before forming p_L. The plotted ranges are −17 to 17 in α/r_g and −12.5 to 12.5 in β/r_g.

Polarization scale. The color scale spans 0% to 1% in steps of 0.2 percentage points. The dark central mask excludes pixels below 1.5% of the peak baseline intensity, where the fractional polarization is sensitive to the small denominator.

Reading the maps together. The three-dimensional view in (c) shows the same observable over the central field with a separate color range and intensity mask. The right-hand map retains the image-plane coordinates for direct comparison with the brightness distribution on page 1.

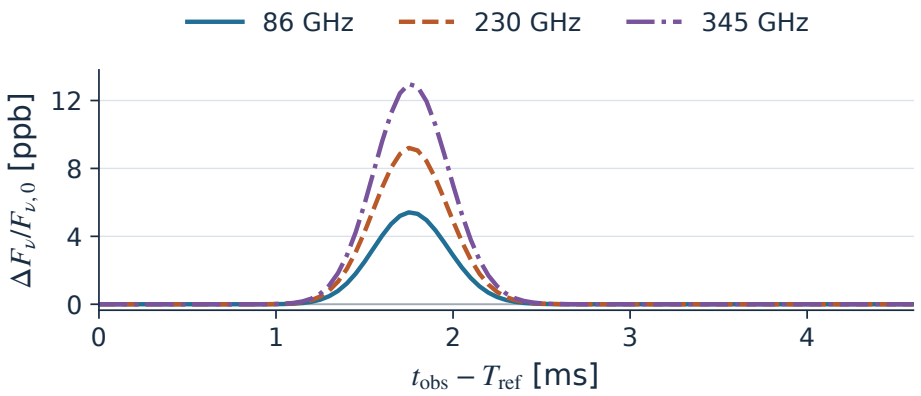
Time-dependent polarimetric response and identifiability of localized energy deposition in irradiated Kerr plasmas

Jingxu Wu[1] · Zhengnan Zhang[2] (presenter) · Xiatong Li[3]

[1,2,3] Lomonosov Moscow State University, Moscow, Russia

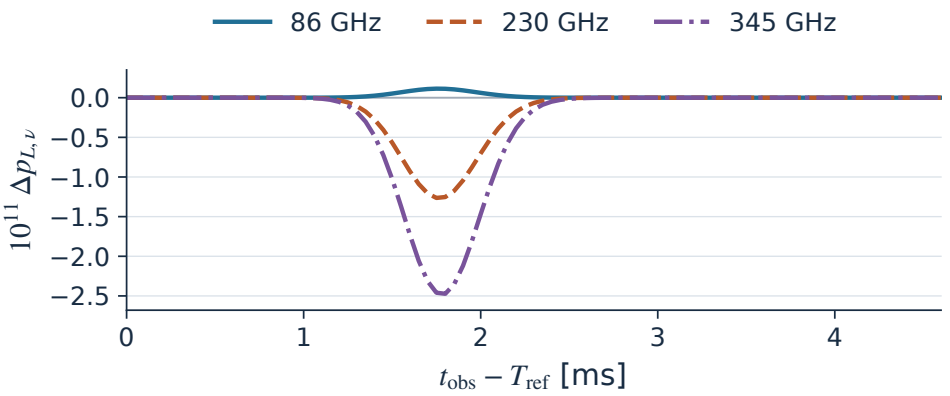
[1] wuxj@my.msu.ru · [2] n2994208@gmail.com · [3] be2312701251@gmail.com

Multi-frequency flux response



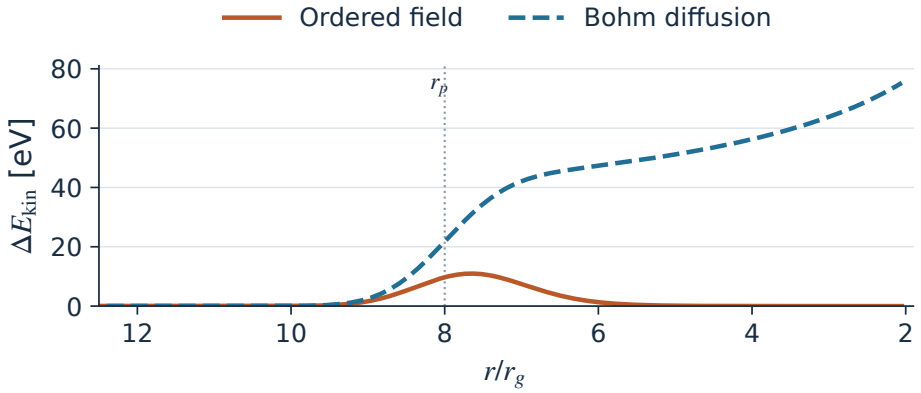
Matched pulse response. The ordinate is the screen-integrated flux change $\Delta F_\nu/F_{\nu,0}$ in ppb (10^{-9}). All bands use the same 192 × 192 ray grid, ordered-field escape and no-pulse reference at each frequency.

Multi-frequency linear polarization response



Net linear polarization. We integrate I, Q and U over the image before forming $p_{L,\nu} = \sqrt{(Q^2 + U^2)}/I$ from the integrated Stokes values. The ordinate gives the pulse-minus-baseline change in units of 10^{-11}.

Lepton energy response along the central streamline



Energy retained in the lepton spectra. ΔE_{kin} is the change in total lepton kinetic energy per initial electron. The dotted line marks the pulse center. The ordered-field response peaks at 10.96 eV near 7.68 r_g, and the Bohm response reaches 75.27 eV at the inner boundary.

Response peaks and arrival times

ν [GHz]	Baseline p_L [%]	Peak $\Delta F/F_0$ [ppb]	Flux peak [ms]	$10^{11}\,\Delta p_L$ at $\lvert\Delta p_L\rvert$ peak	Pol. peak [ms]
86	0.0077	5.41	1.75	+0.11	1.75
230	0.0918	9.21	1.75	-1.26	1.75
345	0.1997	12.97	1.75	-2.47	1.80

Peak definition. Times are measured relative to T_{ref} on a 0.05 ms grid. The polarization value keeps its sign at the maximum absolute response.

Grid check. The 128^2 to 192^2 change is at most 0.0019% for flux and 2.9% for polarization, measured by the largest curve difference relative to each 192^2 peak magnitude.

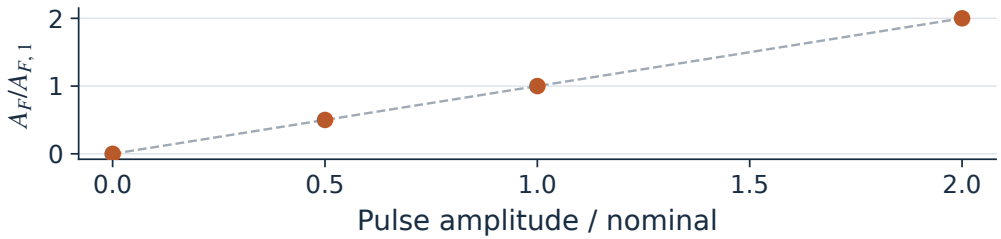
Time-dependent polarimetric response and identifiability of localized energy deposition in irradiated Kerr plasmas

Jingxu Wu[1] · Zhengnan Zhang[2] (presenter) · Xiatong Li[3]

[1,2,3] Lomonosov Moscow State University, Moscow, Russia

[1] wuxj@my.msu.ru · [2] n2994208@gmail.com · [3] be2312701251@gmail.com

Response to pulse amplitude



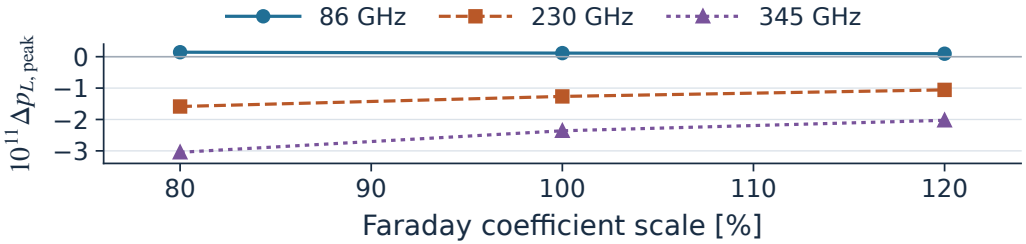
230 GHz pulse scaling. A_F is the peak relative flux response and $A_{F,1}$ is its nominal value. The linearized kinetic model follows the dashed reference and returns zero for zero input.

Camera-grid convergence

ν [GHz]	Flux peak change [%]	Linear polarization peak change [%]
86	0.0007	0.17
230	0.0008	0.20
345	0.0020	5.21

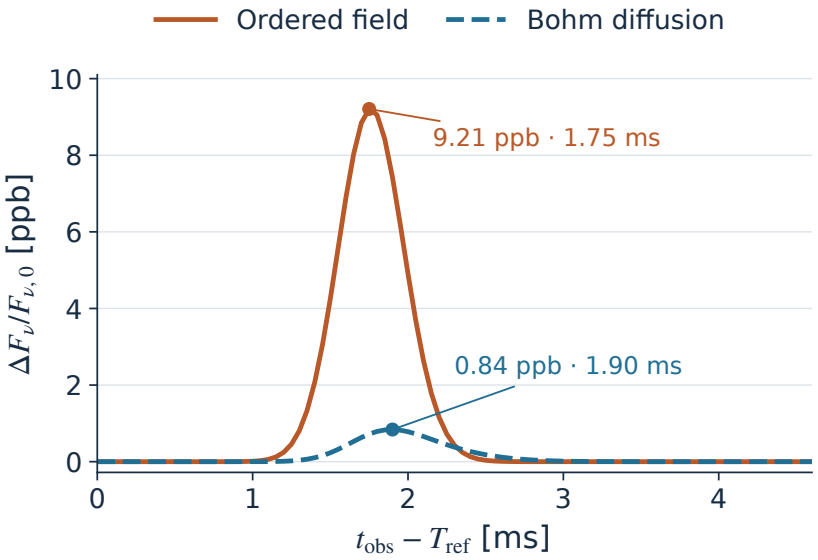
192² versus 288² rays. Peak differences are relative to the 288² values, using the same 0.0125 ms sampling near the pulse. The response sign is preserved at all three frequencies.

Sensitivity to Faraday coefficients



Joint rescaling. We scale Faraday rotation and conversion together. The signed extrema retain their signs, with up to 29% change in magnitude.

Escape prescription and the 230 GHz flux response



230 GHz PULSE RESPONSE UNDER TWO ESCAPE PRESCRIPTIONS. The ordered-field and Bohm-diffusion models use the same incident beam, Gaussian energy input and 192 × 192 ray grid. Each curve is the pulse-minus-baseline flux divided by its own no-pulse flux.

Peak amplitude and timing. Ordered-field streaming peaks at 9.21 ppb at 1.75 ms, while Bohm diffusion peaks at 0.84 ppb at 1.90 ms. The two arrival times use the same reference and a 0.05 ms sampling interval.

Comparison in common flux units. The no-pulse Bohm flux is 1.81 times the ordered-field flux. After converting the relative peaks to common flux units, the Bohm peak increment is 16.5% of the ordered-field increment.

Connection to the lepton response. On the central streamline (page 3), Bohm diffusion retains a larger kinetic-energy perturbation toward the inner boundary. The observed flux weights contributions from the full image through emission, absorption, redshift and photon travel time. The radial density taper also suppresses the contribution at the inner edge.

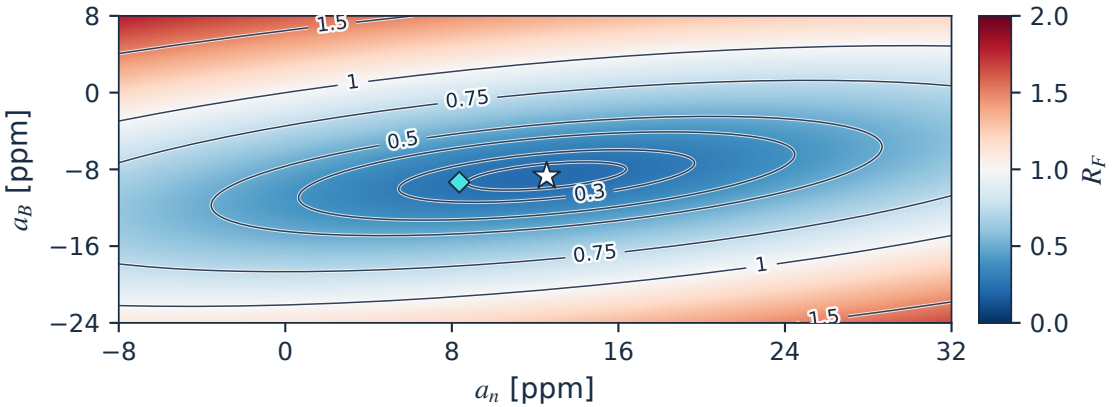
Time-dependent polarimetric response and identifiability of localized energy deposition in irradiated Kerr plasmas

Jingxu Wu[1] · Zhengnan Zhang[2] (presenter) · Xiatong Li[3]

[1,2,3] Lomonosov Moscow State University, Moscow, Russia

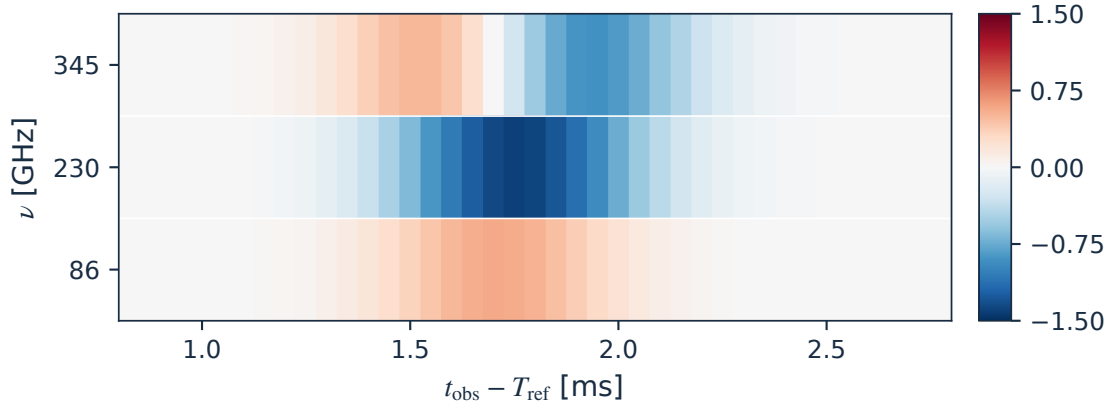
[1] wuxj@my.msu.ru · [2] n2994208@gmail.com · [3] be2312701251@gmail.com

Flux-only fit in density–field amplitude space



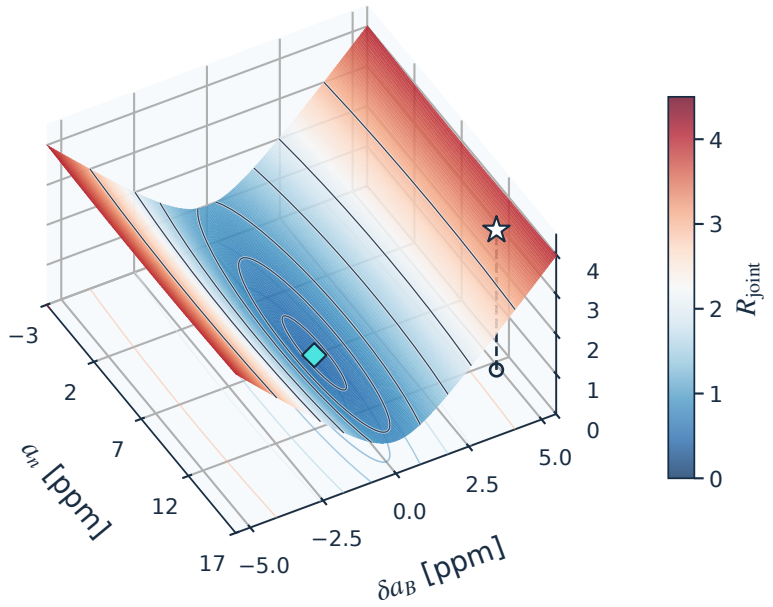
Flux-only mismatch. The white star marks the flux-only fit and the cyan diamond marks the joint fit. The expanded amplitude range contains the full $R_F = 0.50$ contour. The minimum R_F is 0.227.

Where the polarization residual remains



Signed residual after the joint fit. Each row shows the heating-minus-fit difference δp_L at one frequency. Blue is negative and red is positive. The image shows the pulse window, while the fit uses the full 0–4.6 ms time series.

Joint fit of flux and linear polarization



CAN DENSITY AND FIELD CHANGES MIMIC HEATING? The controls use the deposition source's Gaussian envelope and fix the spectral shapes, flow and field direction. Their peak fractional changes are a_n and a_B.

Valley coordinates. The field axis shows $\delta a_B = a_B - a_B^*(a_n)$, where a_B^* minimizes the joint residual at fixed density amplitude. Height and color show $R_{joint} = \sqrt{[(R_F^2 + R_L^2)/2]}$. Each block residual is normalized by the L^2 norm of its heating target across all bands and times.

Best joint fit. At $a_n = +8.36$ ppm and $a_B = -9.33$ ppm (cyan diamond), $R_{joint} = 0.495$. The fit leaves 25% of the flux norm and 65% of the polarization norm as residuals. The white star shows the flux-only fit on the joint surface. Its dashed guide ends at the open circle on the base plane.

Model scope. The surface uses first-order response templates. The 192^2 camera gives $R_{joint} = 0.591$, compared with 0.495 on the plotted 288^2 camera. The polarized templates and fit amplitudes remain resolution-sensitive.

Time-dependent polarimetric response and identifiability of localized energy deposition in irradiated Kerr plasmas

Jingxu Wu[1] · Zhengnan Zhang[2] (presenter) · Xiatong Li[3]

[1,2,3] Lomonosov Moscow State University, Moscow, Russia

[1] wuxj@my.msu.ru · [2] n2994208@gmail.com · [3] be2312701251@gmail.com

Main findings

Multi-frequency response to localized heating.

The ordered-field relative flux peaks are 5.41, 9.21 and 12.97 ppb at 86, 230 and 345 GHz. Near 1.8 ms, the integrated linear polarization fraction rises at 86 GHz and falls at 230 and 345 GHz. Flux adds across the image, while Stokes Q and U can cancel before the polarization fraction is formed. The signs persisted when both Faraday coefficients were rescaled to 80% and 120% of their baseline values.

Escape changes the observable response.

Bohm diffusion retains more excess kinetic energy along the central streamline and carries it farther inward. At 230 GHz the flux response peaks at 1.75 ms for ordered-field escape and 1.90 ms for Bohm diffusion. The Bohm increment is 16.5% of the ordered-field increment in common flux units. The image integrates emission through a tapered density profile, with absorption, redshift and travel delays.

A joint density–field fit leaves a polarization residual.

On the 288 × 288 camera, fitting only the flux leaves 22.7% of its target norm. The joint fit allows the amplitudes of both controls to vary under the same Gaussian envelope. It leaves 25.5% of the flux norm and 65.2% of the polarization norm, so the frequency and timing structure of the polarization residual provides additional evidence.

Scope of the conclusions

Model comparison.

The two controls change the local density normalization and field strength in the transfer coefficients, with fixed spectral shapes, flow and field direction. To test a broader set of alternatives, allow the onset, duration and spatial extent to vary, and compare the best fits after refining the polarized templates.

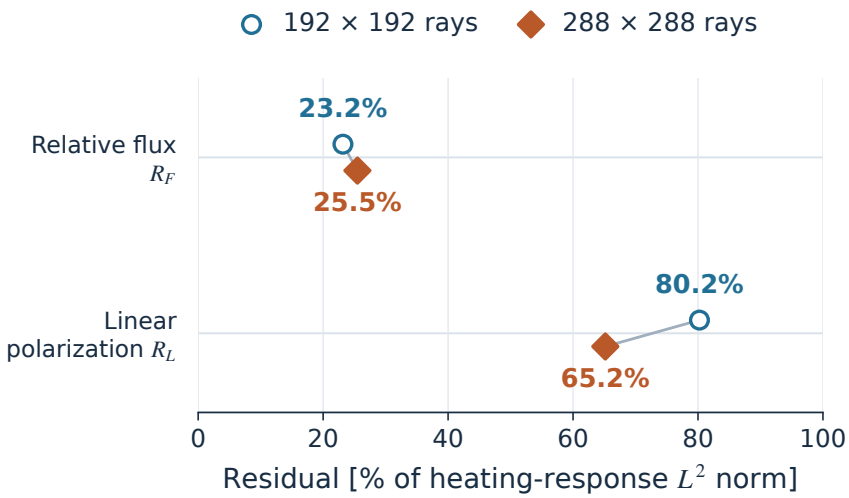
Observational detectability.

The residual chart weights the flux and polarization blocks equally. To estimate detectability, sample the model curves at the instrument's cadence, apply its noise model, and include intrinsic plasma variability. Compare all alternatives under the same observing conditions using the resulting uncertainty in each observable.

Reaction attribution.

The ^{56}Fe(γ,n)^{55}Fe channel motivates an energy scale for the prescribed pulse. Testing its contribution requires propagating the reaction products, computing the energy they deposit in the leptons, and comparing matched simulations with the channel enabled and disabled at the same incident irradiation.

Residual evidence across camera grids



RESIDUALS AFTER A JOINT FIT. Each camera has its own best joint fit. The points show the relative L² mismatch of the fitted controls to the heating target, pooled over the three frequencies and all fitted times. Each percentage is the residual norm divided by the heating-response norm for that same observable.

Resolution dependence. The joint residual is 0.591 on the 192² camera and 0.495 on the 288² camera. Both grids leave a larger relative residual in linear polarization than in flux, although the polarized templates and fit amplitudes remain sensitive to resolution.

Where the mismatch remains. On the 288² camera, the 230 GHz polarization residual is negative around the pulse. The 345 GHz residual changes sign across the pulse window. These patterns show which parts of the time series the joint fit misses.

WHAT THE POLARIZATION ADDS

Multi-frequency linear polarization reveals a substantial mismatch after fitting the tested density and field changes to the prescribed heating response.